High Frequency Kink Interaction in Vertically Vibrated Granular Media

Matt Jones
Evanston Township High School

November 17, 2004

1 Problem Statement

In this research, new kink patterns on piles of granular materials (specifically, bronze powder) vertically vibrated at frequencies between 140 and 360 Hz are presented. This paper reports the results of physical experimentation attempting to determine the cause of these patterns. It documents the interactions that occur at the previously-unexamined frequencies in this range, further exploring the growing field of granular materials.

2 Purpose

Granular materials, a subset of particulate materials identified by their lack of interparticulate attraction [1], are a presence in everyday and industrial life, from sand at the beach to pills and capsules in the pharmaceutical industry [2]. Their action and interaction are relatively poorly understood, and thus they are an area of increasing research.

Granular research has been conducted in a number of different areas, and the following research concentrates on one: vertical vibrations. Because granulars constitute a highly dissipative system, a constant input of energy is necessary to keep them in motion. In this case, that energy comes from oscillating the surface on which they lie. Different types of patterns have been observed under different conditions when vibrated vertically, and are discussed in Section 4.

In this instance, preliminary experimentation using vertically vibrated bronze powder revealed the formation of an intriguing pattern on a pile at frequencies exceeding 140 Hz. The pattern started as a straight line kink (shear line between two period–doubled regions in opposite phase) on a preformed pile, and became gradually more complex, rotating and doubling back upon itself (Figure 1). Period–doubled regions are areas where grains only come in contact with the driving container every other cycle. The following research was conducted to discover the conditions under which this phenomenon occurred and to deduce its cause.

Figure 1: Three pictures of the pattern as it progresses taken from frame captures in ambient incandescent down lighting. Approximately 8 seconds between pictures.

Past research has not identified such a pattern, nor has it identified anything that interacts with itself in such a way. This self interaction, to be discussed further in Section 7, is characteristic of the observed, reproducible pattern.

3 Rationale

Because there are so many possibilities for the use of granular materials, research needs to be done to examine how they act. Specifically, vertical vibrations and the resulting phenomena are relevant in that they have potential applications involving self-assembly (heap formation), mixing, and segregation [3]. They also, under certain conditions, have the potential to enhance mixing or segregating operations. Therefore, it is necessary to understand as much possible about the actions of vertically vibrated granular media. This research strives to document and describe one phenomenon in an unexplored realm and aid the comprehension of others in the process.

4 Background

Granular materials have applications throughout industry. They are present as raw materials such as grains, produce, ores, and sand; and as powders or capsules in the

medical, pharmaceutical, and chemical industries [1]. Because of their widespread use, there is a significant demand to understand better how granulars behave under varying circumstances.

Granular materials sometimes exhibit properties similar to liquids, but other times exhibit completely different properties. For example, when vertically vibrated, granulars exhibit many similarities to liquids, except for phase-dependent phenomena. Granulars can develop regions with different phase, while a liquid's viscosity prevents this [4]. Also, when "mixed" with a tumbler, different-sized elements such as peas and rice will often segregate and form bands, rather than combining to provide an even distribution as would be the case with liquid. This segregation has become a problem, as the pharmaceutical industry depends on adequate mixing for precise manufacturing and, ultimately, the safety of its customers. A court decision has dictated that production of pharmaceuticals must be halted if inadequate or incomplete mixing occurs [2]. Many studies have been conducted in the fields of mixing and segregation, but there is still much to learn.

Past research with regard to vibrations has looked at what interactions occur when a sample of granular materials is excited by a vertical vibrator. Such research has implications in the realms of granular research, including mixing, segregation, and self-assembly. Vertical vibrations, in particular, have been studied under various conditions. Pattern formations depend on a number of factors, including layer depth, vibration frequency, maximum acceleration Γ, and the presence of air. See Figure 2 for examples.

The three factors varied in this experiment are frequency, layer depth, and Γ, where

$$\Gamma = \frac{A \cdot (2\pi \cdot f)^2}{g} = \frac{a_{max}}{9.81 \frac{m}{s^2}} \tag{1}$$

where g is the acceleration due to gravity, A is the amplitude of oscillation of the container, f is the frequency of oscillation, and a_{max} is the maximum acceleration of the container.
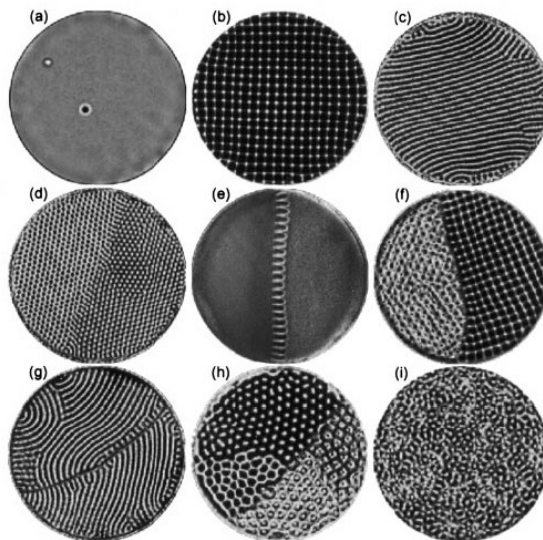

Figure 2: A few examples of patterns in vertically vibrated granular media [2].

It is when this variable, Γ, exceeds 1 that most patterns occur, because for $\Gamma > 1$, the peak downward acceleration of the container exceeds that of gravity. Because the grains are neither cohesive nor adhesive to the container, they cannot accelerate downward faster than driven by gravity, and thus leave the bottom surface for part of the downward stroke. Certain Γ values at a given frequency allow regions of different phase to develop, and result in the formation of and transition between different patterns.

The majority of research that has been done with vertical vibration patterns has been in the lower frequencies, under about 60 Hz. Little examination has been made of higher-frequency patterns that form above 150 Hz. Additionally, all studies have incorporated thick, rigid containers that are resistant to vertical or horizontal deflection. Such a control yields a simpler situation, but also prevents some more complex patterns from forming. However, for the present investigation, a flexible container is necessary, as the pattern does not form without it.

Granular research with inherently non-rigid containers is often based on Chladni plates driven by standard electromechanical shakers to form Chladni patterns. These patterns occur when a flexible sheet, usually steel, is vibrated at frequencies that yield nodes within the boundaries of the sheet, as illustrated in Figure 3. A node is an area with vertical displacement of zero, while its surrounding areas have nonzero amplitudes [5]. When sand is sprinkled on a vertically vibrated Chaldni plate, it is vibrated into the areas with zero displacement and stays there, as there is no force to move it out.

337 Hz   849 Hz   4098 Hz   337Hz Fixed at one Point   337Hz Fixed at two Points

Figure 3: Pattern formation on vertically vibrated Chladni plates, thickness .092 cm, diameter 28.95 cm. Red dots indicate points held stationary during vibration.

While these simple Chaldni patterns were not present in the pattern, the concept of nonuniform vibration contributed to the pattern's formation, as it did not occur when the plate was made more rigid (See Section 7).

5   Materials

The granular material used was bronze powder with claimed diameters ranging from 90 μm to 150 μm and actual diameters measured with a micrometer ranging from 50 μm to 150 μm. It was obtained from AcuPowder [6]. The volume was measured using a plastic 10mL graduated cylinder, and the bottom was tapped to settle the powder. Volumes used ranged from 7 mL to 13 mL. The powder was placed in a Petri dish with an inner diameter of 8.92 cm. The Petri dish was super glued either directly to the shaker's shaft or to a banana plug which then fit into the shaker's shaft. The middle of the Petri dish was determined in both cases by drawing lines to connect each of three equally spaced points around the dish and drawing the perpendicular bisectors to two sides of the resulting equilateral triangle. The point of intersection of these perpendicular bisectors was used as the middle of the dish.

The shaker was driven by a Pasco Scientific PI-9587C digital function generator and amplifier set to output a sine wave at a given frequency with 5 significant figures of precision (2 decimal places when used in the 100—999 range).

Because Γ was such an important parameter in the observation of phenomena, it was necessary to measure it. Some previous experiments have measured the approximate amplitude of the shaker and differentiated twice with respect to time to find the maximum acceleration [7]. This method, while simple, is rather time consuming, degenerates for non-sinusoidal oscillation, and does not work for higher frequencies with considerable Γ values but immeasurable amplitudes. Others have used a more exact method, employing accelerometers to measure the acceleration directly. Due to their increased accuracy, precision, and time efficiency, accelerometers were used. Analog Devices supplied four ADXL210JE dual-axis analog & digital output accelerometers [8]. One was mounted directly to the shaft, and the remaining three were attached to the underside of the Petri dish (Figure 4). Attachment was made using superglue and stuck-together metal paper staples to

facilitate mounting parallel to the axis of sensitivity but perpendicular to the Petri dish. Zip ties were used to minimize cable rattling and uneven weighting that could alter the dish's movement (Figure 5).
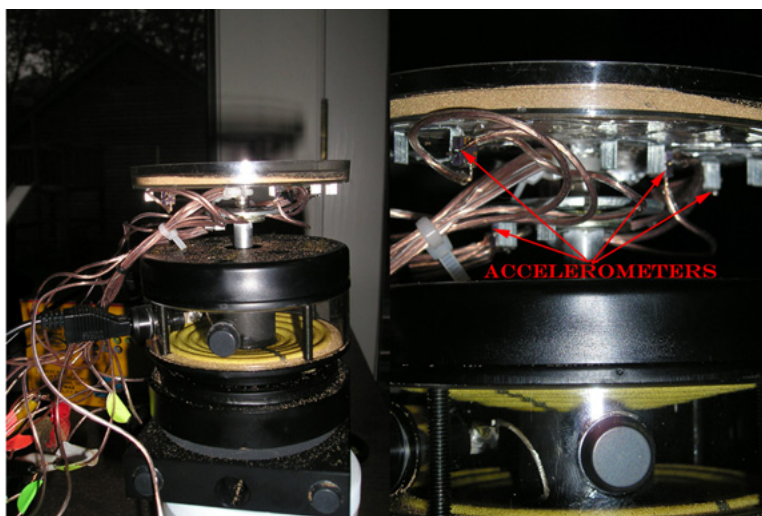

Figure 4: The shaker and Petri dish assembly attached via banana plug, showing accelerometer mounts.

The accelerometers were prepared by soldering 24-gauge copper speaker wires to their power, common, analog y-axis, and, for two of them, the digital y-axis and digital duty cycle period-adjusting pin. However, the digital output was only used briefly, and discontinued when it was determined that the analog would be more versatile. The analog output's peak to peak voltage could be measured, and its signal could be put into a computer using the sound card. All accelerometers were powered by two AA batteries in series, providing between 2V and 3V DC between each power and common pin. They were all calibrated at the beginning of a new day's test run.

Each accelerometer put out a voltage that varied linearly with respect to the acceleration. The output was connected to an oscilloscope calibrated to vary the beam one division per .5 volts. This allowed measurement of peak–peak (p-p) voltage to a precision of $\pm.05$V p-p, amounting to between 4% and 22% precision.
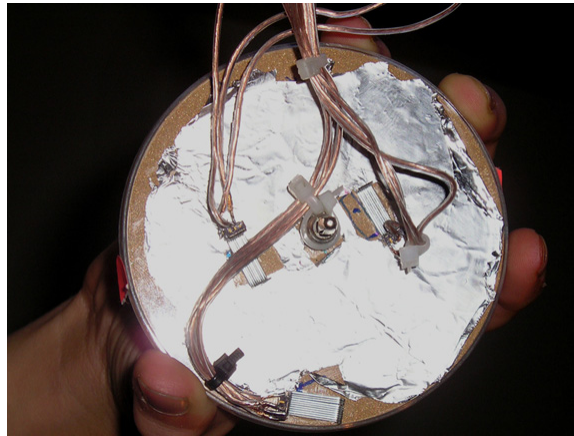
Figure 5: The bottom of the Petri dish, showing mounting of accelerometers, banana plug, and aluminum foil for static electricity dissipation.

Sweep time was varied to best observe the waveform and p-p voltage. For Fast Fourier Transform (FFT) analysis and qualitative recording of the waveform, a Dell Inspiron 8600 laptop computer with the accelerometers' analog output connected to its microphone input was used. The program "Analyzer 2000" was used for both FFT analysis and for waveform observation. Screen captures provided graphic files containing the FFT and waveform data in Figure 10.

Still pictures were taken from video frame captures or a Canon SLR on ASA 100 film, mounted as shown in Figure 6. Lighting for the SLR was provided via flash unit about 15 cm from the side slightly above the level of the dish (about a 10° angle of elevation). Videos were taken with a Sony DCR-TRV240 digital video camera, recording to a Digital8 cassette at NTSC standard 29.97 frames per second. The video was subsequently transferred to a Pentium 4 computer running Windows XP, and frame captures were taken with Adobe Premiere. Lighting for video was provided by either ambient incandescent down lighting, or a spotlight at a distance of about 30 cm and an elevation of about 20°. The video camera was mounted in a similar manner to the still camera in Figure 6.

Figure 6: The camera and shaker setup for taking pictures of the pattern. The SLR is shown, but the video camera was mounted in a similar manner.

6   Methods

Experimentation and observation was carried out with the equipment and construction mentioned in Section 5. The Petri dish was connected to the shaft in one of the two previously discussed manners. A volume of bronze powder was measured and poured into the Petri dish. When the dish was attached directly to the shaft, a pile was made in the middle using a spoon to scrape the powder towards the center. When the dish was attached with a banana plug, tapping the sides in places 180° around the edge moved powder towards the center to form a pile of similar size and proportions to that constructed using the spoon on the fixed plate.

To observe the Γ at which the pattern occurred at a given frequency, first the accelerometers were calibrated. This involved measuring each voltage with the apparatus in its normal position, then turning it upside down, and re-measuring each voltage. As the difference in voltage would be that from 2 times gravity, the following equation was used to calculate the accelerometers' calibration in volts

per G.

$$\frac{Volts}{G} = \frac{V_{up} - V_{down}}{2} \tag{2}$$

Knowing this equation and the peak to peak (p-p) voltage allows for the calculation of Γ. Since the p-p voltage is the difference between maximum upward acceleration and maximum downward acceleration, it must be halved to get only the maximum downward acceleration (Γ).

$$\Gamma = \frac{1}{2} \cdot \frac{2}{V_{up} - V_{down}} \cdot V_{p-p} = \frac{V_{p-p}}{V_{up} - V_{down}} \tag{3}$$

After the accelerometers were calibrated, test runs were conducted. First, a pile was constructed as described above, then the frequency was set on the function generator, and the amplitude slowly increased by hand until the pattern became visible. At this point, the peak-peak voltages of the accelerometers were measured as described in Section 5, starting at the outermost accelerometer and working inwards. Values were recorded and are displayed in Figure 9.

Testing for size segregation was conducted by following the above procedure to create a pile and induce the pattern, then collecting a sample of bronze powder from each region and measuring the diameter of one particle to 10 μm with a micrometer. A total sample of 36 grains was measured, covering two trials.

7 Results

The pattern observed is shown in Figure 7, ranging from its initial appearance as a nearly-linear kink to its state approximately 20 seconds later, as a much wider kink between the two initial regions. The kink is the shear line between the darker regions on either side of it. These darker areas are in opposite phase with frequency $f/2$. In more complex patterns (Figure 8), there exist multiple kinks and therefore multiple period-doubled regions around them.

It was determined that this kink pattern occurs most prominently on a pile of bronze powder ranging in diameter from approximately 6 to 7 cm, with a compacted volume ranging between 7 and 13 mL. Through experimentation, it was
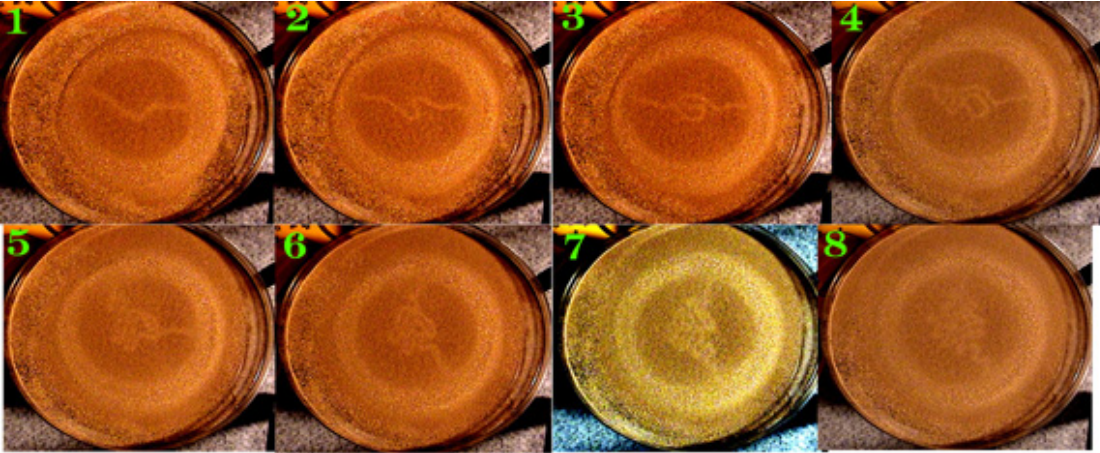
Figure 7: A progression of the pattern over about 20 seconds, taken from video shot with overhead lighting only.

determined that the pattern occurred at frequencies ranging from 140 Hz to 360 Hz, and for Γ between 5 and 10 (Figure 9). The pattern is most pronounced at frequencies in the middle of this range (180 Hz to 290 Hz), though it appears to some degree for all frequencies between 140 Hz and 360 Hz. With higher Γ, the kink gets more complex, even spawning separate, circular kinks and eventually degenerating at $\Gamma > 9$.

The period doubling phenomenon that caused the kink was confirmed in two ways. As shown in Figure 10, there was a sub harmonic (frequency $f/2$) component of the acceleration waveform for both the sensor under one darker region and the one on the driving shaft. This implies that there was an impact with a granular layer once every two peaks of the driver. Since one region was larger, it made a larger impact, thus causing the $f/2$ peak in 10B. Additionally, video of the two regions driven at 181.15 Hz was shot at 29.97 frames per second (the NTSC standard) with a fast shutter speed. This yielded a periodic change in color between the two regions (indicating a change from fluidized to solidified state) approximately every 23 frames, or .77 seconds. Assuming instantaneous frames (possible because a fast shutter speed was used), $\frac{oscillation}{framerate} = \frac{181.15}{28.87} = 6.044$. There-
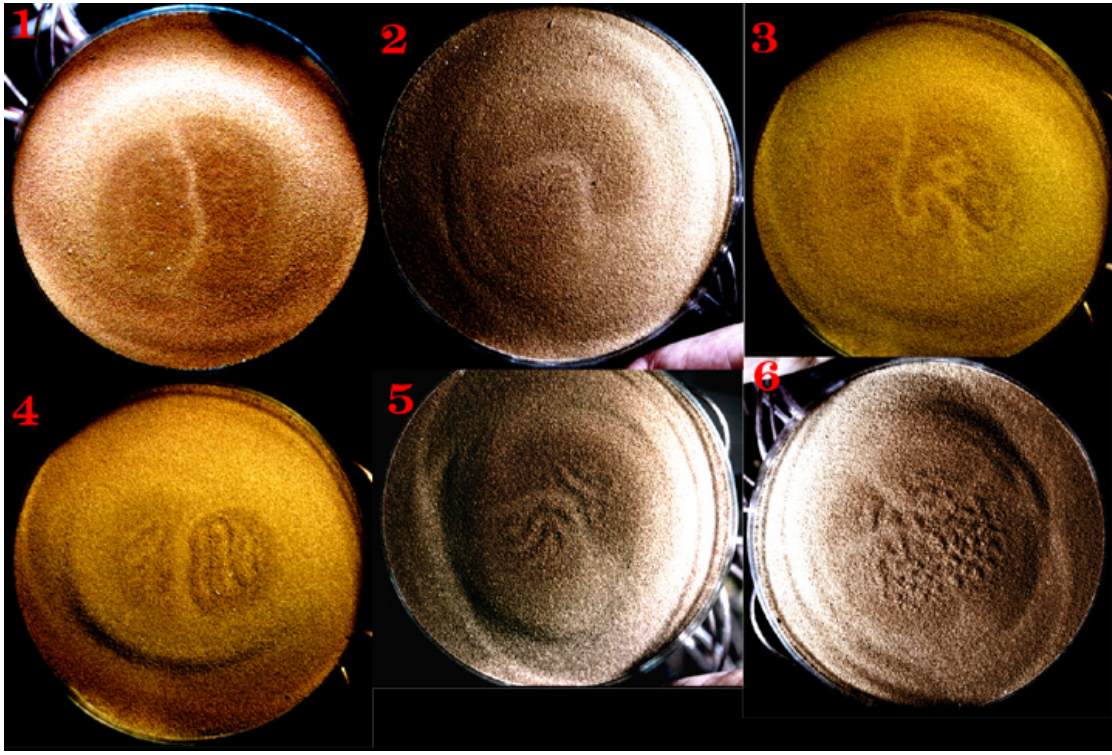
11

Figure 8: Different variations of the initial pattern, appearing at different Γ values. 1. A simple straight kink. 2. A $\cup$-shaped kink. 3. An S-shaped kink with a circular kink to the side. 4. A straight kink at higher Γ, exhibiting stripe patterns in the period-doubled regions. 5. A $\cup$-shaped kink with stripe patterns in the period-doubled regions. 6. Two $\cup$-shaped kinks with stripe patterns in the period-doubled regions.

fore, the shaker hit a peak 6 times between each frame, with a shift of .044 period at the next frame. Since $.044^{-1} = 22.73 frames = \frac{22.37}{29.97} sec = .76 sec$, it took 22.72 frames = .76 seconds to capture the whole oscillator waveform. This shows that the two regions are in opposite phase.

The kink occurred most prominently when it was on a pile of powder, with a maximum grain depth of 30-50 layers. If the oscillator was started under the same conditions that produced the kink, but with a relatively flat distribution of powder as opposed to a pile, either a weaker pattern or random, chaotic stripes and
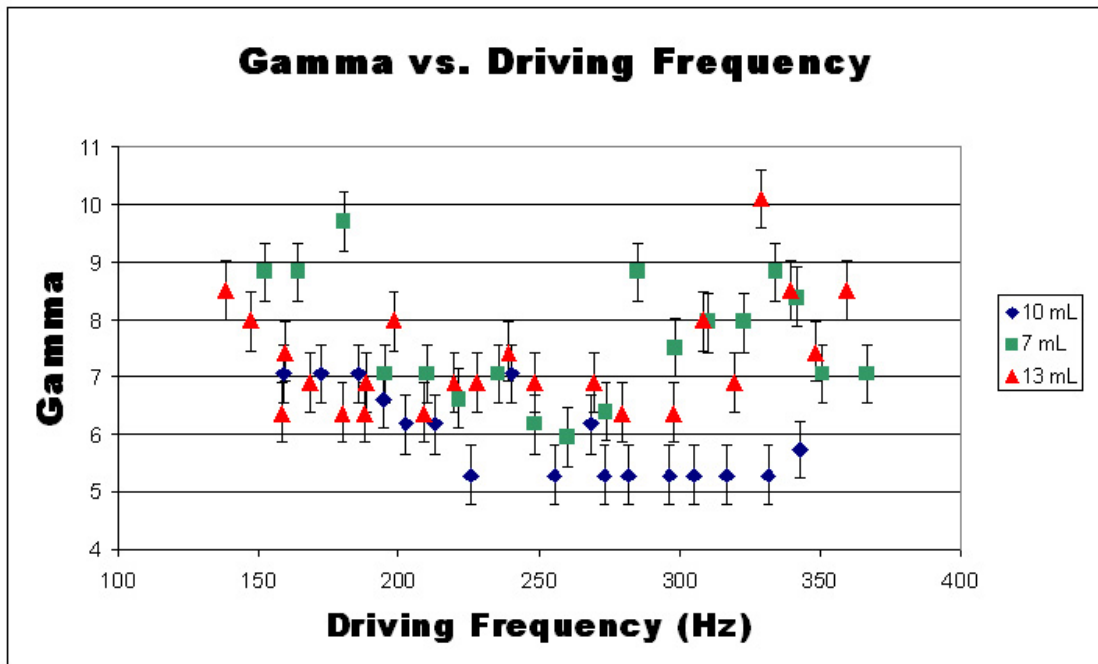
Figure 9: A chart of frequency vs. Γ for points at which the pattern first appears with Γ increasing from 0. Different colors signify different volumes, as noted on the legend at right. Error bars come from error in measuring p-p voltage as described in Section 5.

localized kinks were observed. Similarly, as the vibrator was run for a period of time, the bronze avalanched down the pile, eventually flattening out and resulting in diminished sharpness or considerable kink width, as shown in Figure 7.

The pattern was first observed with the Petri dish attached to the shaker using a banana plug. It was glued to the dish on a hexagonal mounting surface with longest diagonal 9mm and apothem 4mm (total area .52 cm^2). This allowed some dish flex and instability. Therefore, control for dish flex seemed desirable, and was accomplished by attaching the dish directly to the shaker. This direct attachment was achieved using a pile of washers with outer diameter 31.5 mm (total area 10.5 cm^2) leveled and glued to the shaker shaft and the bottom of the Petri dish. However, when the dish was fixed but the other conditions kept constant, only
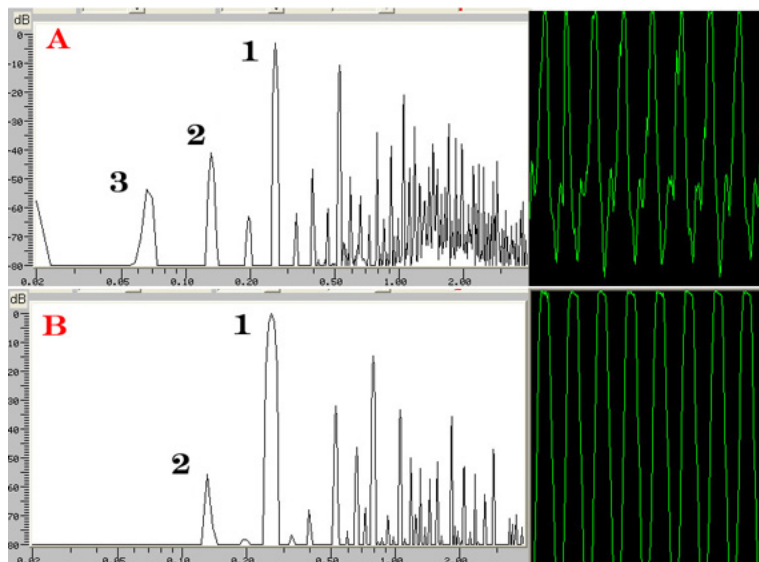
13

Figure 10: FFT graphics and waveform examples with driving frequency (1) and subharmonic peaks (2,3) which indicate period doubling. Figures are for A, an accelerometer under one region near the kink and B, the driving (shaft) accelerometer. The FFT diagram is on a logarithmic frequency scale, with decibels on the y-axis.

chaotic patterns emerged. Thus, it was shown that a somewhat flexible plate was necessary for pattern formation. Further experimentation was carried out using the initial banana plug attachment.

Evidence of vertical size segregation, the Brazil-nut effect [9], appeared when a few grains of sand approximately .8mm in diameter serendipitously fell into the Petri dish, and filtered to the top almost immediately. This phenomenon is commonly-known in vertically vibrated granular media, and it is logical that it would appear in this case.

8   Discussion

The formation of kinks has previously been observed, usually starting at $\Gamma > 5$, for frequencies larger than about 37 Hz [3]. Their formation is an inherent feature

of granular materials, and does not depend on outside factors like air or dish sidewalls, as heaping and other phenomena do. Other research with regard to kinks has looked at their boundary frequencies and Γ values. There is little research available for vertical vibrations with frequencies exceeding 100 Hz, but those that discuss kinks at lower frequencies all agree that they begin to appear at about $\Gamma = 5$ [9, 3, 4].
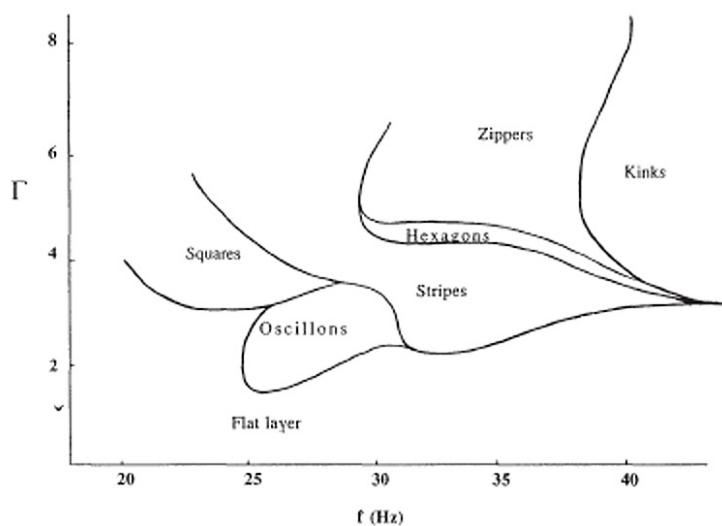

Figure 11: A phase diagram for .15-.18mm brass spheres with layer depth 20, collected with decreasing Γ. [3]

However, the only kink interaction studied previously was at the frequency boundary between patterns, as the kink made a transition to a "zipper" (Figures 11, 2e). There has been no previous evidence of kinks interacting with themselves to form complex nonlinear patterns as I have discussed. Such interaction could be used in conjunction with previous research into size-segregation using kinks [9] to further segregate particles without frequency modulation.

9   Future Prospects

Further research could be done to better determine the cause of these patterns. One factor to test is if the pattern occurs when the same setup is run in the absence of air. As the pattern is based on kinks, which are not caused by interaction with the surrounding gas, experimenting in a vacuum would be expected to yield the same results. It should nonetheless be tested. Additionally, a computer model would prove particularly useful, as it has in similar research [9]. It would give further insight into the cause of the pattern, its dynamic nature, and what is actually happening on the granular scale.

Additionally, further research with the same conditions but different Petri dishes, or even platforms of a different material would help to explain the container flexibility's role in the pattern formation. Similarly, a variation in grain size, density, and material would uncover the relationship between the size of the material and the pattern size. It would also be relevant to conduct similar research to that in [9] with regard to the possibilities of horizontal grain segregation.

10   Acknowledgements

I would like to thank my physics teacher, Dr. Mark Vondracek, who helped me get started on this project and helped me periodically throughout it. He provided me with almost all of the equipment used, and was very helpful in proofreading and formatting. I would also like to thank Professor Paul Umbanhowar, of Northwestern University, who met with me on numerous occasions to give me an overview of granulars, told me what sorts of phenomena could be investigated, helped give my research direction, and was a wonderful help with proofreading the paper. I would also like to thank my parents for being so supportive, helping me proofread, and putting up with a table full of equipment in their house for six months. Lastly, Analog Devices was very kind to send me six accelerometers free of charge.

Bibliography

[1] J. Feda, *Mechanics of particulate materials: the principles*. New York: Elsevier Scientific Pub. Co., 1982.

[2] H. M. Jaeger, T. Shinbrot, and P. B. Umbanhowar, "Does the Granular Matter?," *PNAS*, vol. 97, no. 24, 2000.

[3] P. K. Das and D. Blair, "Phase boundaries in vertically vibrated granular materials," *Physics Letters A*, no. 326-328, 1998.

[4] F. Melo, P. B. Umbanhowar, and H. L. Swinney, "Hexagons, Kinks, and Disorder in Oscillated Granular Layers," *Physical Review Letters*, vol. 75, no. 21, 1995.

[5] J. Nolen, "Chladni Figures and Vibrating Plates." November 10, 2004. Online, Internet at http://www.phy.davidson.edu/StuHome/jimn/Java/modes.html.

[6] "Bronze Powders." November 10, 2004. Online, Internet at http://www.acupowder.com/pdf/bronze.pdf.

[7] D. Summerhays, "Vertically Vibrated Granular Media: A Study of Oscillon and Wave Patterns in Bronze Powder." Intel Science Talent Search Submission. Available http://facweb.eths.k12.il.us/chemphys/science_research_papers.htm, 2002.

[8] "Analog Devices: ADXL210: Product Page." November 10, 2004. Online, Internet at http://www.analog.com.

[9] S. J. Moon, D. I. Goldman, J. B. Swift, and H. L. Swinney, "Kink-Induced Transport and Segregation in Oscillated Granular Layers," *Physical Review Letters*, vol. 91, no. 13, 2003.